Supporting Information

Tao et al. 10.1073/pnas.1407743111

SI Text

Methods. This involves a series of chemical-free processes including shadow mask deposition for the Mg resistor and coils, thin-film casting for the silk substrates, and low-temperature embossing (Fig. 1 *A* and *B*). Briefly, the Mg serpentine resistor was fabricated on a silk substrate of ∼50-μm thickness with a resistance of ∼300 Ω, determined by the metal thickness (i.e., ∼200 nm). After the deposition of MgO as a 1-μm passivation layer, a 6-turn receiving Mg coil (∼2 μm) was deposited through a second deposition step to connect and power the serpentine resistor.

Materials. The bacteria strains used were *E. coli* and *S. aureus* ATCC 25923 (American Type Culture Collection). Bacterial culture dishes, BD brand Tryptic Soy Broth, and Tryptic Soy Agar were purchased from Fisher Scientific.

Silk Solution Preparation. Silk fibroin aqueous solutions were prepared as previously described. Briefly, *Bombyx mori* cocoons were boiled for certain period ranging from 15 to 60 min (varying with different applications and lifetime of devices), in an aqueous solution of 0.02 M sodium carbonate, followed by a thorough rinse using DI water. After 2 d drying in a chemical hood, the silk fibroin was dissolved in an aqueous solution containing 9.3 M lithium bromide at 60 °C for 4 h. The solution was then injected in Slide-a Lyzer dialysis cassettes (MWCO 3500, Pierce) and was dialyzed against DI water for 48 h (8 water changing in an interval of 6 h). The final concentration of the silk fibroin was roughly 6 wt %, which was determined by drying 1 mL of as-prepared silk solution in an oven of 60 °C overnight and measuring the weight of the final product–film. Molecular mass distribution: 171–460 kDa for 15-min boiled silk (15_mb); 31–268 kDa for 30-min boiled silk (30_mb); and 31–171 kDa for 60-min boiled silk (60_mb).

Silk Film Preparation. The silk solution was cast on a flat surface (i.e., the bottom of polystyrene Petri dishes) and was left drying at ambient conditions for 12 h, resulting in silk fibroin films. The thickness of silk film can be precisely controlled by adjusting the volume and concentration of the silk solution and the casting area. For example, a dose of 0.2 mL/cm^2 of 6 wt % silk solution produces films ∼100 μm thick.

Ampicillin-Doped Silk Films Preparation. Sodium ampicillin (A9518, Sigma-Aldrich) was dissolved in MilliQ water (wt/vol = 50 mg/mL) at 4 °C and then mixed with regenerated silk fibroin solution to obtain a solution made of 60 mg/mL silk fibroin and of 10 mg/mL sodium ampicillin. Antibiotic-loaded silk fibroin films (SF-AB) were then obtained by solvent casting.

Silk Film Postprocessing. Silk fibroin films are water-soluble. Certain processes can render the film water-insoluble. In this work, three methods were used. (*i*) Water annealing (for producing silk substrates on which the devices were fabricated): The silk films cast on silicon substrates (which were pretreated to be hydrophobic for easy peeling off after device fabrication) were placed in a water-filled vacuum desiccator. The vacuum pump was switched on for ∼5 min to fill the desiccator chamber with vapor. The vacuum was then turned off to let the homogeneous water vapor anneal the silk films–samples. A minimum of 3 h vapor annealing was used to ensure the silk films did not dissolve in water. Longer annealing time increases the crystallinity within the films, resulting in slower degradation once implanted. (*ii*) Methanol annealing (for producing silk films for device encapsulation): The soluble silk films were immersed in 80% (vol/vol) methanol solution for a certain period (ranging from 5 min to 1 h) to increase beta-sheet content within the films. (*iii*) Thermal annealing (for producing silk film for device encapsulation): The soluble silk films were thermal-treated using a house- built embosser. The embossing time, pressure, and temperature profile determine the crystallinity of the silk films, which determine the lifetime of the as-encapsulated devices.

Device Encapsulation Using Thermal Embossing–Lamination. Thermal embossing–lamination technique was used in this work for thermal control of silk fibroin film crystallinity. Moreover, with reflow upon heating, silk can act as a glue by controlling its thermal state.

Bacteria Culture. Lyophilized *S. aureus* and *E. coli* cultures were reconstituted and expanded according to instructions provided by ATCC. To test susceptibility, bacteria cultures were grown in liquid Tryptic Soy Broth for 18–24 h to an optical density (OD_{600}) between 0.8 and 1 (corresponding to a viable count of approximately 10^7–10^8 CFU per mL).

In Vitro Zone of Inhibition Testing. In vitro antibacterial effect was estimated by using the Kirby–Bauer Susceptibility Test, where antibacterial effect is assessed by comparing zones of clearance in bacterial lawns. Briefly, 50 μL of the *S. aureus* culture were plated on Tryptic Soy Agar plates. The devices were placed on a primary coil for wireless powering–heating. The heating temperature was controlled by adjusting the input power of the primary coil using an IFI Sccx100 RF amplifier and a commercial IR camera (FLIR SC645). The treated plates were incubated overnight at 37 °C to allow lawn growth. After 24 h the zone of inhibition was measured and analyzed using ImageJ image analysis software.

s.c. *S. aureus* Infection in Vivo Studies. Male BALB/c mice weighing 20–25 g were shaved on the back and depilated with Nair (Carter-Wallace Inc.). Mice were anesthetized with an injection of ketamine–xylazine mixture (90 mg/kg ketamine, 10 mg/kg xylazine) for surgery and infection. The operative area of skin was cleaned with alcohol, and the silk devices were implanted s.c. on the shaved back of each animal. Five μL of diluted bacteria culture containing ∼2×10^5 CFU of *S. aureus* were dropped on top of the silk devices and implanted together with the device. Wireless heating treatments were performed at different temperatures (42 and 49 °C) for 10 min. During the 10 min of thermal application the animals were kept under anesthesia. After 24 h, animals were anesthetized and tissues at the implantation site and surrounding area were excised and transferred to sterile 50-mL Falcon tubes containing 10 mL of sterile Dulbecco's phosphate buffered saline for further processing. The mice were then euthanized by carbon dioxide asphyxiation. All animal studies were conducted under protocols reviewed and approved by Tufts University IACUC protocols.

Tissue Homogenization and Bacteria Counting. Excised tissue samples were weighed and homogenized using a T25 basic Ultra Turrax mechanical homogenizer (IKA Works, Inc.). Bacteria in the homogenate were estimated by standard plate count methods. Colonies were counted after 24 h of incubation at 37 C. The bacterial count was expressed as the number of CFU per wound. To normalize for variability among the mice, CFU counts for each treatment modality were divided by the CFU count measured for the untreated wound and reported as a percentage.

Antibiotic Release. Heat-stimulated ampicillin release was investigated as a function of silk fibroin molecular weight and polymorphic structure. To obtain silk fibroin with varying molecular mass, cocoon degumming time was set to 15, 30 and 60 min, to obtain protein with a molecular mass in the range of 171–460 kDa, 31–268 kDa, and 31–171 kDa, respectively (1). In addition, the degree of silk fibroin crystallinity was modulated to ~15%, 24%, and 33% by adjusting the time of the water-vapor annealing process to 3, 6, and 12 h, respectively (2). Antibiotic release from heat-stimulated silk films was then investigated by heating ampicillin-loaded silk films to 50 °C for 10 min in PBS (10 mg of film per mL of buffer) and then measuring ampicillin release adapting a previously reported protocol (1). In brief, 1 mL of PBS was added to each sample, which was then incubated at 37 °C. At desired time points (1, 3, 6, 12, 24, and 48 h), the buffer was removed and replaced with fresh buffer. The amount of released compound was determined using UV-vis spectroscopy at 230 nm. The amount of released antibiotic in each sample was summed with the amounts at each previous time point to obtain cumulative release values. Three samples were tested ($n = 3$) and each sample was assayed in triplicate.

Statistical Analysis. Antibiotic release data were compared with one-way ANOVA test with a Tukey means comparison implemented with software Origin Pro v.8 (OriginLab).

Estimation of Mg Level of Each Device. The amount of Mg can be calculated based on design layout and thickness of a Mg heater. The calculated amount of Mg used for a resistor (~200 nm) and a spiral coil (~2 μm) is 0.35 and 26.43 μg, respectively, resulting in a total mass of Mg of 26.79 μg.

Mg Ion Level Measurements Using ICP-AES. Freshly harvested mouse skin samples of similar dimension–weight were weighed, dried at 60 °C overnight, and then weighed again to determine the amount of dry solid mass in the tissue. Skin samples were then dissolved for 12 h in HCl 6M (Sigma-Aldrich). The same stock solution was used to dissolve all of the different samples to avoid possible interbatch difference in ion content. The Mg ion levels in each tissue were determined using ICP-AES (Leeman Labs PS-1000). A calibration test and a clean cycle were applied for each measurement to avoid cross-contamination.

Histology. To assess the safety of the heating procedure and the degradation process of the implanted devices, we examined histological slices of tissues surrounding the implanted devices. Samples were dehydrated through a series of graded alcohols, embedded in paraffin, and sectioned with slices having an approximate thickness of 10 μm. Sections were stained with H&E.

1. Pritchard EM, Hu X, Finley V, Kuo CK, Kaplan DL (2013) Effect of silk protein processing on drug delivery from silk films. *Macromol Biosci* 13(3):311–320.

2. Hu X, et al. (2011) Regulation of silk material structure by temperature-controlled water vapor annealing. *Biomacromolecules* 12(5):1686–1696.

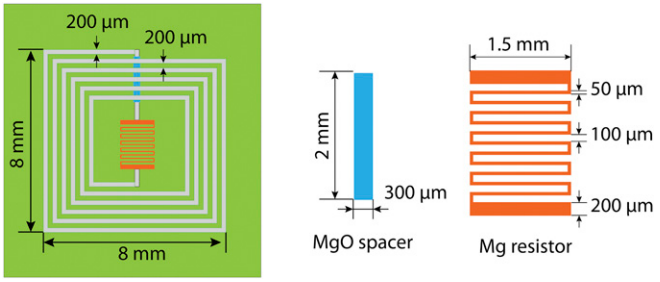

Fig. S1. Geometries and dimensions of the device used in the experiment.

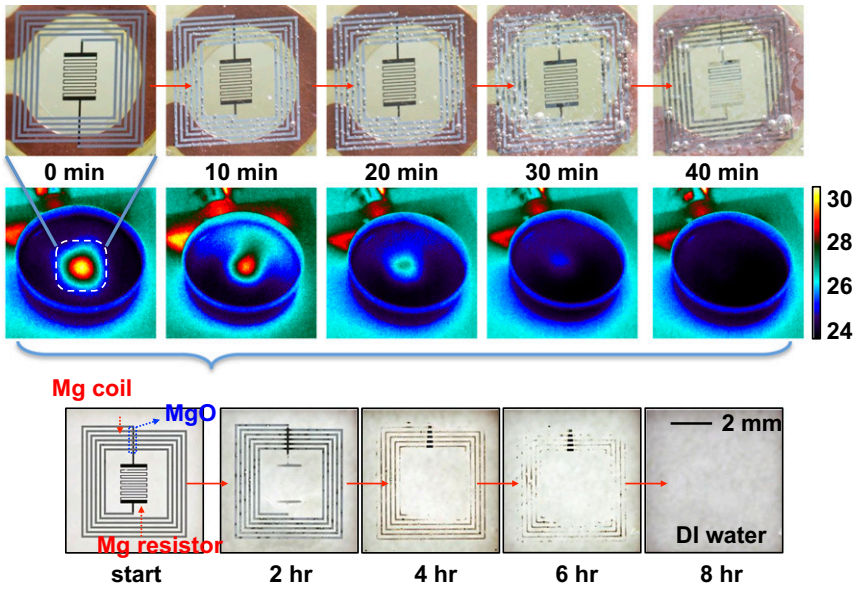

Fig. S2. Optical (and the corresponding IR) images of the dissolution of a device (consisting of a Mg serpentine resistor and a powering coil, fabricated on a glass substrate) in PBS at room temperature to illustrate the in vitro degradation process of individual Mg components.

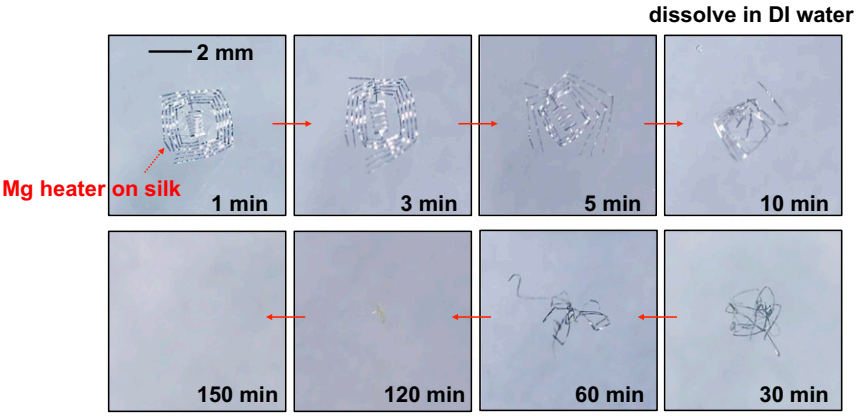

Fig. S3. Optical images of full dissolution of the bare device (i.e., without any encapsulation layer) in DI water at room temperature over a time interval of 2.5 hours.

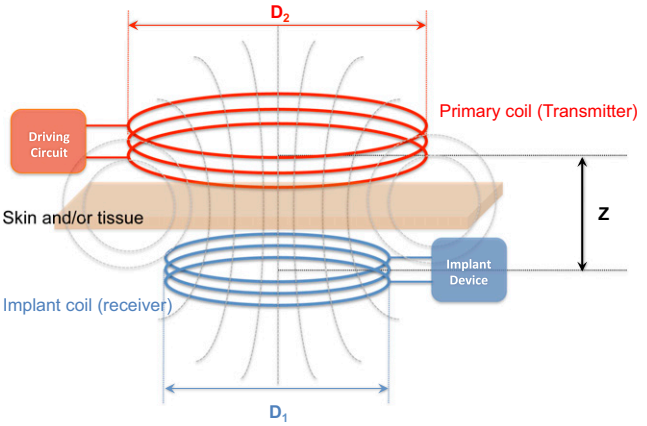

Fig. S4. Schematics of induction coupling between the primary coil and the receiver (i.e., implanted) coil for wireless power delivery.

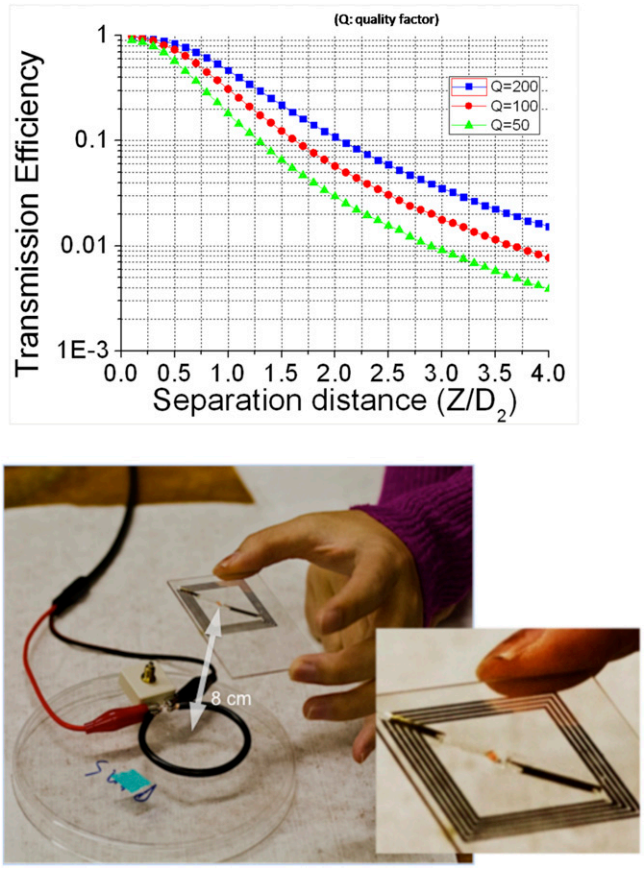

Fig. S5. (*Top*) Calculated wireless transmission efficiency as a function of distance between two coils. (*Bottom*) Example of wireless operation of LED at a distance of ~8 cm from the primary coil. (*Inset*) Detail of the functioning LED.

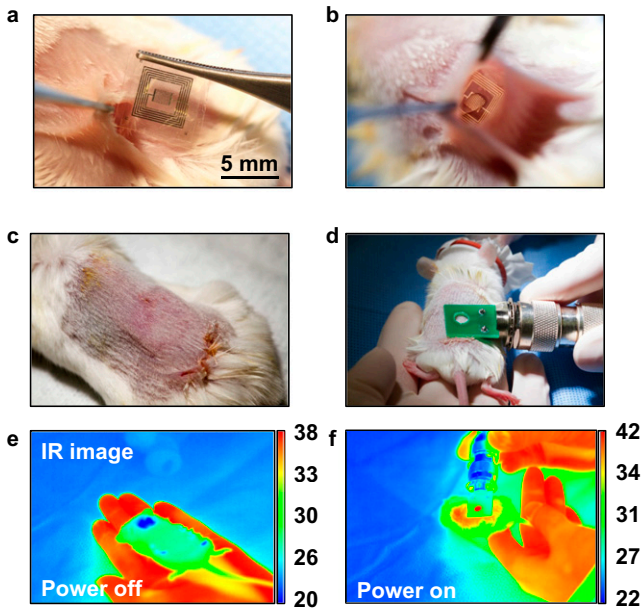

Fig. S6. Images of the device before and after implantation. IR pictures of the implanted device before and after applying the rf power.

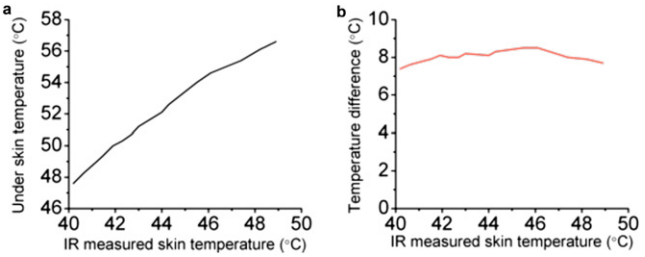

Fig. S7. Temperatures detected on the animal skin by the IR camera; the actual temperatures under the skin were measured to infer the actual temperature experienced at the implant site. The temperatures at the implant site were measured by using a thermocouple placed onto the device that was covered by a piece of mouse skin. The measured temperatures under the skin at the implant site were found to be ~7 °C higher than the values recorded by the IR camera (i.e., skin temperatures).

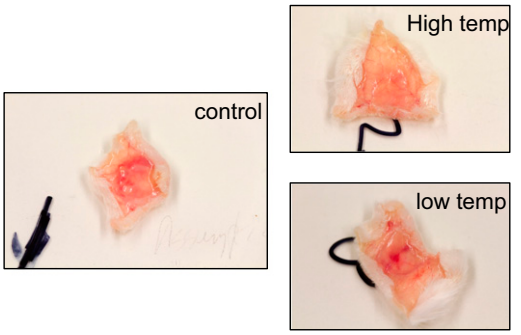

Fig. S8. Optical images of the excised tissues after the infection and thermal treatments. (*Left*) No thermal treatment was applied. Obvious infection as observed, as indicated by the presences of redness and pus. (*Right, Top*) Ten-min treatment at ~57 °C, labeled as high temp; no obvious signs of infection were found. (*Right, Bottom*) Ten-min treatment at ~49 °C, labeled as low temp; signs of infection were found, e.g., the presence of redness.

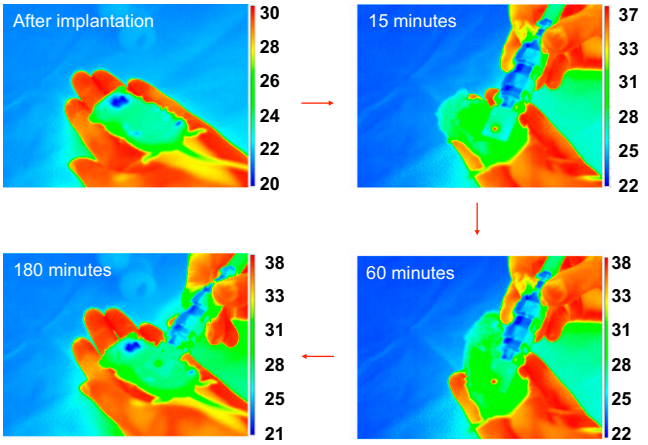

Fig. S9. IR images showing that the implanted device (for the assessments of the device degradation and Mg tracking purpose) started degrading within a time frame of 3 h, as indicated by a decrease of the device's thermal performance (i.e., temperature) when inductively activated by the same amount of RF power.

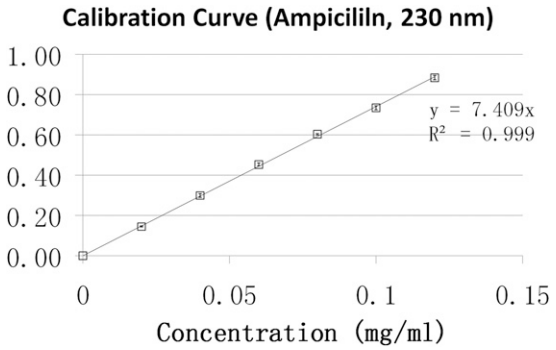

Fig. S10. Bacterial inhibition curve of *Thermos aquaticus* (Catalog: ATCC 25105) at different concentration of ampicillin.

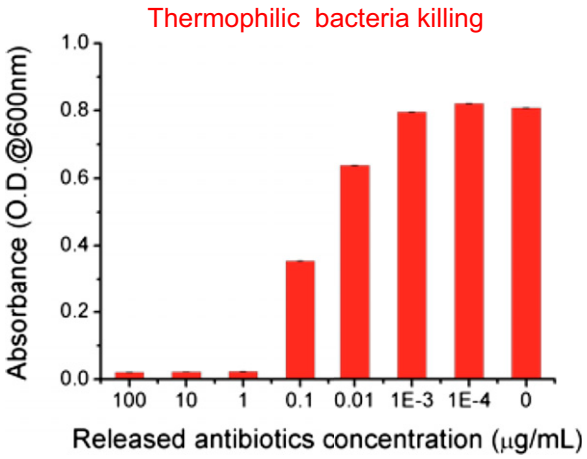

Fig. S11. Efficacy of the wirelessly released ampicillin was evaluated by adding aliquots (~10 μL) of the collected and diluted ampicillin-containing solutions to bacterial cultures (~2 mL) containing *S. aureus* (Fig. 4*C*), *E. coli* (Fig. 4*D*), respectively, and *T. aquaticus* that can tolerate high temperatures usually above 70 °C and measuring the optical density of grown bacterial cultures after 18 h of incubation at 37 °C (Fig. S9).

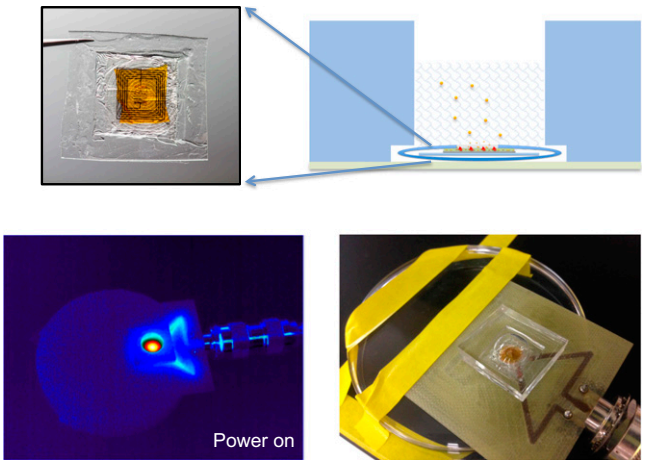

Fig. S12. Device stayed intact and still functional in warm water after 2 weeks.